Generalized gradient approximation for the exchange-correlation hole of a many-electron system

John P. Perdew

Department of Physics and Quantum Theory Group, Tulane University, New Orleans, Louisiana 70118

Kieron Burke

Department of Chemistry, Rutgers University, Camden, New Jersey 08102

Yue Wang

Department of Biostatistics, School of Public Health, University of North Carolina, Chapel Hill, North Carolina 27599-7400

(Received 14 February 1996; revised manuscript received 29 July 1996)

We construct a generalized gradient approximation (GGA) for the density $n_{xc}(\mathbf{r},\mathbf{r}+\mathbf{u})$ at position $\mathbf{r}+\mathbf{u}$ of the exchange-correlation hole surrounding an electron at $\mathbf{r}$, or more precisely for its system and spherical average $\langle n_{xc}(u)\rangle = (4\pi)^{-1}\int d\Omega_{\mathbf{u}}\, N^{-1}\int d^3r\; n(\mathbf{r})n_{xc}(\mathbf{r},\mathbf{r}+\mathbf{u})$. Starting from the second-order density gradient expansion, which involves the local spin densities $n_\uparrow(\mathbf{r}),n_\downarrow(\mathbf{r})$ and their gradients $\nabla n_\uparrow(\mathbf{r}),\nabla n_\downarrow(\mathbf{r})$, we cut off the spurious large-u contributions to restore those exact conditions on the hole that the local spin density (LSD) approximation respects. Our GGA hole recovers the Perdew-Wang 1991 and Perdew-Burke-Ernzerhof GGA's for the exchange-correlation energy, which therefore respect the same powerful hole constraints as LSD. When applied to real systems, our hole model provides a more detailed test of these energy functionals, and also predicts the observable electron-electron structure factor. [S0163-1829(96)04847-3]

I. INTRODUCTION AND SUMMARY OF CONCLUSIONS

Kohn-Sham density functional theory[1-4] would yield the exact ground-state energy E and spin densities $n_\uparrow(\mathbf{r}),n_\downarrow(\mathbf{r})$ of a many-electron system, if the exact exchange-correlation energy functional $E_{xc}[n_\uparrow,n_\downarrow]$ were known. Good results for solids are often found from the local spin density (LSD) approximation[1]

$$E_{xc}^{LSD}[n_\uparrow,n_\downarrow]=\int d^3r\; n(\mathbf{r})\epsilon_{xc}(n_\uparrow(\mathbf{r}),n_\downarrow(\mathbf{r})), \quad (1)$$

where $\epsilon_{xc}(n_\uparrow,n_\downarrow)$ is the known[5] exchange-correlation energy per particle of an electron gas with uniform spin densities $n_\uparrow$, $n_\downarrow$, and $n=n_\uparrow+n_\downarrow$. Equation (1) is clearly valid when the spin densities vary slowly over space, but this condition is *violated* by real atoms, molecules, and solids. Indeed, the next systematic correction in the slowly varying limit, the second-order gradient expansion approximation[6-11] (GEA),

$$E_{xc}^{GEA}[n_\uparrow,n_\downarrow]=E_{xc}^{LSD}[n_\uparrow,n_\downarrow]+\sum_{\sigma,\sigma'}\int d^3r\; C_{xc}^{\sigma\sigma'}(n_\uparrow,n_\downarrow)$$
$$\times\nabla n_\sigma\cdot\nabla n_{\sigma'}/n_\sigma^{2/3}n_{\sigma'}^{2/3}, \quad (2)$$

is less accurate than LSD.[6,12,13]

Gunnarsson and Lundqvist[14] explained the success of LSD as follows: The exchange-correlation energy is the electrostatic interaction of each electron at $\mathbf{r}$ with the density $n_{xc}(\mathbf{r},\mathbf{r}+\mathbf{u})=n_x+n_c$ at $\mathbf{r}+\mathbf{u}$ of the exchange-correlation hole which surrounds it. In atomic units ($\hbar=e^2=m=1$),

$$E_{xc}[n_\uparrow,n_\downarrow]=\frac{1}{2}\int d^3r\; n(\mathbf{r})\int d^3u\; n_{xc}(\mathbf{r},\mathbf{r}+\mathbf{u})/u. \quad (3)$$

See Refs. 14 and 15 for reviews. LSD models the hole density as

$$n_{xc}^{LSD}(\mathbf{r},\mathbf{r}+\mathbf{u})=n_{xc}^{unif}(n_\uparrow(\mathbf{r}),n_\downarrow(\mathbf{r});u), \quad (4)$$

where $n_{xc}^{unif}(n_\uparrow,n_\downarrow;u)$ is the hole density in an electron gas of uniform spin densities $n_\uparrow,n_\downarrow$, for which an accurate analytic model now exists.[15] Thus LSD respects the sum rules

$$\int d^3u\; n_x(\mathbf{r},\mathbf{r}+\mathbf{u})=-1, \quad (5)$$

$$\int d^3u\; n_c(\mathbf{r},\mathbf{r}+\mathbf{u})=0, \quad (6)$$

which constrain the energy integral of Eq. (3). Moreover, Eq. (3) involves only the system and spherically averaged hole density

$$\langle n_{xc}(u)\rangle=\int\frac{d\Omega_{\mathbf{u}}}{4\pi}\frac{1}{N}\int d^3r\; n(\mathbf{r})n_{xc}(\mathbf{r},\mathbf{r}+\mathbf{u}), \quad (7)$$

for which LSD provides a fairly reasonable description.[16]

The LSD hole has other desirable features, such as the negativity condition on the exchange hole[17]

$$n_x(\mathbf{r},\mathbf{r}+\mathbf{u})\leq 0, \quad (8)$$

an accurate[18] (but inexact[19]) on-top value $n_{xc}(\mathbf{r},\mathbf{r})$, and the correct electron-electron cusp condition at $u=0$.[20] GEA improves upon LSD at small u, but displays spurious large-u behavior,[21,17,12,22] which is sampled by the long-range Coulomb interaction $1/u$. Langreth and Perdew[21] showed that the GEA hole, which is a truncated expansion and not the exact hole of any system, violates Eq. (6).

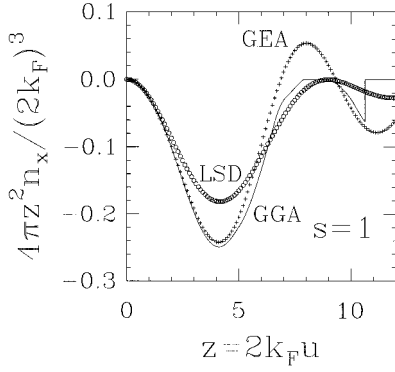Nonempirical generalized gradient approximations (GGA's),[12,23]

FIG. 1. Spherically averaged exchange hole density $n_{\rm X}$ for $s=1$ in LSD (circles), GEA (crosses), and GGA (solid line).

$$E_{\rm xc}^{\rm GGA}[n_\uparrow,n_\downarrow]=\int d^3r \; f(n_\uparrow,n_\downarrow,\nabla n_\uparrow,\nabla n_\downarrow), \qquad (9)$$

often start from the GEA for the hole $n_{\rm xc}^{\rm GEA}$ and cut off its large-u contributions to restore exact conditions such as Eqs. (5), (6), and (8). Since only the system average of Eq. (7) is needed, $\nabla^2 n$ contributions to the GEA are first transformed via integration by parts on $\mathbf{r}$. GGA's may be applied directly or hybridized with exact exchange.[24,25]

In Sec. II, we present our GGA model for the exchange hole. The first such model was that of Perdew and Wang[12] in 1986 (PW86), who used sharp cutoffs on $n_{\rm x}^{\rm GEA}$ to enforce Eqs. (5) and (8), yielding

$$E_{\rm x}^{\rm GGA}[n_\uparrow,n_\downarrow]=\tfrac{1}{2}E_{\rm x}^{\rm GGA}[2n_\uparrow]+\tfrac{1}{2}E_{\rm x}^{\rm GGA}[2n_\downarrow], \qquad (10)$$

$$E_{\rm x}^{\rm GGA}[n]=\int d^3r \; n\,\epsilon_{\rm x}^{\rm unif}(n)F_{\rm x}(s), \qquad (11)$$

where

$$\epsilon_{\rm x}^{\rm unif}(n)=-3k_F/4\pi, \qquad (12)$$

$$k_F=(3\pi^2 n)^{1/3}, \qquad (13)$$

$$s=|\nabla n|/2k_F n. \qquad (14)$$

The real-space cutoff gave a numerical function $F_{\rm x}(s)$ (see Fig. 1 of Ref. 12), which was fitted to an analytic form, $F_{\rm x}^{\rm PW86}(s)$. In the later work of Perdew and Wang[23,26] in 1991 (PW91), Becke's[27,28] semiempirical refinements plus additional theoretical constraints were included in $F_{\rm x}^{\rm PW91}(s)$, although $F_{\rm x}^{\rm PW91}(s)$ was a worse fit to the numerical function than was $F_{\rm x}^{\rm PW86}(s)$. Both the PW86 and PW91 parametrizations were contorted[29] at small s to recover the expected GEA of Eq. (2).

Recently, Perdew, Burke, and Ernzerhof (PBE)[30] presented a simplified construction of a simplified GGA for exchange and correlation, in which all parameters (other than those in LSD) are fundamental constants. Although independent of PW91 or any model for the hole, the PBE functional is numerically equivalent to PW91 for most purposes, and

$$F_{\rm x}^{\rm PBE}(s)=1+\kappa-\kappa/(1+\mu s^2/\kappa), \qquad (15)$$

where $\mu=0.219\,51$ (to preserve the good LSD description of the exchange-correlation energy in the linear response of the uniform gas) and $\kappa=0.804$. In Sec. II, we construct a GGA hole that accurately reproduces Eq. (15), by applying a damping factor to the PW86 exchange hole. The damping factor, used only for exchange, reflects the more pathological large-u behavior of the $n_{\rm x}^{\rm GEA}$, and the "double" nature of its GGA cutoffs, which enforce both Eqs. (5) and (8).

In Sec. III, we present our model for the GGA correlation hole. The first such model,[23] which led to the PW91 correlation energy functional, was based upon sharp cutoffs of crude approximations for both the LSD and gradient contributions to the hole. We refine these crude approximations, but find essentially the same correlation energy, which can be accurately represented by the PBE functional

$$E_{\rm c}^{\rm PBE}[n_\uparrow,n_\downarrow]=\int d^3r \; n\{\epsilon_{\rm c}(r_s,\zeta)+H^{\rm PBE}(r_s,\zeta,t)\}, \qquad (16)$$

where

$$r_s=(3/4\pi n)^{1/3}, \qquad (17)$$

$$\zeta=(n_\uparrow-n_\uparrow)/n, \qquad (18)$$

$$t=|\nabla n|/2k_s\phi n, \qquad (19)$$

$$\phi=\tfrac{1}{2}[(1+\zeta)^{2/3}+(1-\zeta)^{2/3}], \qquad (20)$$

$$k_s=(4k_F/\pi)^{1/2}, \qquad (21)$$

$$H^{\rm PBE}=\gamma\phi^3\ln\left\{1+\frac{\beta}{\gamma}t^2\left[\frac{1+At^2}{1+At^2+A^2t^4}\right]\right\}, \qquad (22)$$

$$A=\frac{\beta}{\gamma}[\exp\{-\epsilon_{\rm c}^{\rm unif}/\gamma\phi^3\}-1]^{-1} \qquad (23)$$

and $\gamma=0.031\,091, \beta=0.066\,725$. The reduced gradients s and t measure how fast $n(\mathbf{r})$ is varying on the scales of the local Fermi wavelength $2\pi/k_F$ and the local Thomas-Fermi screening length $1/k_s$, respectively.

In Ref. 30, Eq. (22) was derived from three limits:

$$H^{\rm PBE}\to\beta\phi^3 t^2 \qquad (t\to 0), \qquad (24)$$

$$H^{\rm PBE}\to-\epsilon_{\rm C}^{\rm unif} \qquad (t\to\infty), \qquad (25)$$

and

$$E_{\rm c}^{\rm PBE}[n_{\uparrow\gamma},n_{\downarrow\gamma}]\to{\rm const} \qquad (\gamma\to\infty), \qquad (26)$$

where $n_{\sigma\gamma}(\mathbf{r})=\gamma^3 n_\sigma(\gamma\mathbf{r})$ is a uniformly scaled density.[31] These limits also emerge naturally from the real-space cutoff construction of Sec. III, as shown in Ref. 32. The high-density limit of Eq. (26) is violated by both LSD and PW91.[33]

Thus the PBE correlation energy functional of Eq. (16) can be derived *either* from various limits, as in Ref. 30, or from a real-space construction of the GEA correlation hole, as in Sec. III. The PBE exchange energy functional of Eq. (15) is derived from its limits in Ref. 30, and is then used to improve the real-space cutoff of the GEA exchange hole in Sec. II.

Sharp cutoffs produce a ''choppy'' $n_{xc}^{GGA}(\mathbf{r},\mathbf{r}+\mathbf{u})$ (e.g., see the GGA exchange hole in Ref. 34), but are smoothed in the system and spherical average of Eq. (7). In Sec. IV, we describe the general features of the GGA holes.

We conclude the following: (1) The PW91 and PBE exchange-correlation energy functionals correspond to a GGA exchange-correlation hole, with the known correct features of the LSD hole, plus additional correct inhomogeneity effects. These functionals should therefore perform as reliably as LSD, except under special conditions (see below). (2) The GGA system-averaged exchange-correlation hole of Eq. (7) can be constructed for any system via the formulas given in this work. The coupling-constant integration

$$\langle n_{xc}(u)\rangle = \int_0^1 d\lambda \langle n_{xc,\lambda}(u)\rangle \qquad (27)$$

can be undone, as in Refs. 35 and 15, to extract the physical exchange-correlation hole at full coupling strength ($\lambda = 1$), for comparison with the results of accurate wave-function calculations. (3) The system-averaged hole at full coupling strength is an observable, since its Fourier transform is essentially the electron-electron structure factor $S(k)$ measured in quasielastic scattering processes. We expect the GGA to make a useful prediction for this observable.

Finally, the PW91 and PBE functionals yield great improvements over LSD for the total energies of atoms (and their separate exchange and correlation contributions) or atomization energies of molecules,[26,36–40] but have a mixed history of successes and failures for solids.[41–51] This may be because the exchange-correlation hole can have a diffuse large-u tail in a solid, but not in an atom or small molecule, where the density $n(\mathbf{r})$ itself is well localized. As we shall see in Sec. II, a sharp radial cutoff corresponds to $\kappa = 0.804$ in Eq. (15), while a more diffuse cutoff leads to a smaller value of κ. This uncertainty is also reflected in the PBE derivation of Eq. (15), in which κ is set to the maximum value allowed by the Lieb-Oxford bound[23,52] on E_{xc}.

II. EXCHANGE HOLE

The exact exchange hole arises from the Kohn-Sham noninteracting wave function (a Slater determinant) and satisfies the spin-scaling relation

$$n_x[n_\uparrow,n_\downarrow](\mathbf{r},\mathbf{r}+\mathbf{u}) = \sum_\sigma \frac{n_\sigma(\mathbf{r})}{n(\mathbf{r})} n_x[2n_\sigma](\mathbf{r},\mathbf{r}+\mathbf{u}). \qquad (28)$$

Thus we need only model $n_x[n](\mathbf{r},\mathbf{r}+\mathbf{u})$, the exchange hole as a functional of the density for a spin-unpolarized system.

We write

$$n_x^{GEA}(\mathbf{r},\mathbf{r}+\mathbf{u}) = -\tfrac{1}{2}n(\mathbf{r})y, \qquad (29)$$

where

$$y(z,\mathbf{s},\hat{\mathbf{u}}) = J(z) + D(z)\{4L(z)\hat{\mathbf{u}}\cdot\mathbf{s}/3 - 16M(z)(\hat{\mathbf{u}}\cdot\mathbf{s})^2/27$$
$$- 16N(z)s^2/3\}. \qquad (30)$$

Here $\hat{\mathbf{u}} = \mathbf{u}/u$, $\mathbf{s} = \nabla n/2k_F n$, and

$$z = 2k_F u \qquad (31)$$

is the reduced electron-electron separation on the scale of the Fermi wavelength. The functions $J(z)$, $L(z)$, $M(z)$, and $N(z)$ are known, oscillating functions of z, given in Eqs. (8)–(11) of Ref. 12, respectively. $D(z)$ is a damping factor, which equals 1 at the pure GEA level. To first order in u, $n_x^{GEA} = -n(\mathbf{r}+\mathbf{u})/2$, so that the GEA hole is deeper on the high-density side of the electron.

In our generalized gradient approximation (GGA), the hole is represented as

$$n_x^{GGA}(\mathbf{r},\mathbf{r}+\mathbf{u}) = -\tfrac{1}{2}n(\mathbf{r})y\,\theta(y)\,\theta(u_x(\mathbf{r})-u), \qquad (32)$$

where $\theta(x) = 1$ for $x > 0$ and 0 for $x < 0$. The first step function on the right enforces the negativity condition of Eq. (8), while the second involves a cutoff separation u_x chosen to enforce the normalization condition of Eq. (5), which becomes

$$-\frac{1}{12\pi}\int_0^{z_x} dz\ z^2 y_{sph\,av}(z,s) = -1, \qquad (33)$$

where $z_x = 2k_F u_x$ and

$$y_{sph\,av}(z,s) = \frac{1}{4\pi}\int d\Omega_{\mathbf{u}} y(z,\mathbf{s},\hat{\mathbf{u}})\theta(y(z,\mathbf{s},\hat{\mathbf{u}})). \qquad (34)$$

Equation (33) determines z_X as a function of s, and Eqs. (3) and (11) yield

$$F_x(s) = \frac{1}{9}\int_0^{z_X} dz\ z y_{sph\,av}(z,s). \qquad (35)$$

The angular integration over $\Omega_{\mathbf{u}}$ in Eq. (34) is performed analytically (as explained at the end of this section) and the z integrations of Eqs. (33) and (35) are performed numerically.

As discussed in Refs. 17 and 12, the GEA exchange hole displays an undamped $\cos(2k_F u)$ oscillation as $u \to \infty$. We damp this oscillation by taking

$$D(z) = 1/[1 + (bz)^q] \qquad (36)$$

in Eq. (30). To preserve the GEA hole at small u, $q \geq 2$. Since the LSD hole density is essentially confined to the region $0 \lesssim z \lesssim 2\pi$, and the GEA breaks down when the GEA hole density is much greater than the LSD density, we expect $b \sim 1/2\pi$. The choices $q = 2.5$ and $b = 1/2\pi$ provide a good fit to $F_x^{PBE}(s)$ of Eq. (15).

Figure 1 is a plot of $-y_{sph\,av}(z,s)z^2/12\pi$, appearing in Eq. (33), as a function of z for $s = 1.0$, for the LSD hole and the damped GEA and GGA holes. For large z, the damped GEA hole displays unphysical oscillations about $n_x = 0$. The GGA hole is sharply cut off at $z_x \sim 10.5$, to satisfy Eq. (33), and is identically zero for $8 \lesssim z_x \lesssim 9$, due to the negativity cutoff in Eq. (34). Elsewhere, the GGA hole is not equal to the damped GEA hole because of the step function inside the spherical average in Eq. (34), which produces derivative discontinuities as a function of z, e.g., at $z \sim 7$.

Figure 2 shows numerical results for the reduced cutoff radius z_x as a function of s. As $s \to 0$, the cutoff radius moves out to ∞, and the GGA hole reduces to the damped GEA hole. As $s \to \infty$, the cutoff radius slowly approaches zero, and the hole becomes highly localized around the electron. For

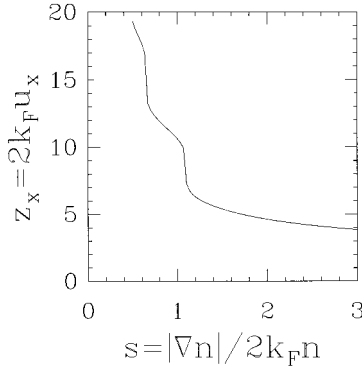FIG. 2. Reduced cutoff separation for the GGA exchange hole as a function of reduced density gradient. For $s \gtrsim 3$, we find $u_x \lesssim r_s$.

intermediate s, the steps in $z_x(s)$ occur where the normalization cutoff passes through a negativity cutoff.

Figure 3 shows various numerical results for the enhancement factor $F_x(s)$ over local exchange as a function of s in the physical range[53] $0 \lesssim s \lesssim 3$, as defined by Eq. (35), as well as the PBE enhancement factor of Eq. (15), with which it agrees closely. We also present the numerical GGA enhancement factor resulting from (1) a diffuse radial cutoff factor $[1 + (u/u_x)^2] \exp[-(u/u_x)^2]$, with u_x fixed by Eq. (33), which leads to a smaller $F_x(s)$ for $s \gtrsim 1$, and (2) with sharp radial cutoffs but with no damping [i.e., $D = 1$ in Eq. (36)], which leads to a slightly larger $F_x(s)$, and a *linear* dependence on s as $s \to 0$. Thus the real-space cutoff procedure determines the general features of $F_x(s)$, but not its exact behavior, which must then be fixed by other constraints [as has been done in the construction of the PW86,[12] PW91,[23] and PBE (Ref. 30) exchange functionals].

We close this section with a technical point: the analytic result for the angular integral in Eq. (34). Let ν be the cosine of the angle between **u** and **s**. Then

$$y_{\text{sph av}} = \frac{1}{2} \int_{-1}^{1} d\nu (A\nu^2 + B\nu + C) \theta(A\nu^2 + B\nu + C), \qquad (37)$$
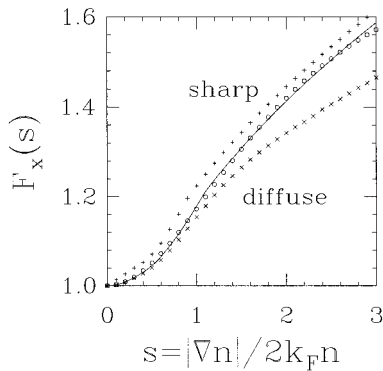

FIG. 3. Enhancement factor over local exchange as a function of reduced density gradient. The solid line is the damped numerical GGA of Eq. (35), the open circles are the PBE of Eq. (15), the pluses are the numerical results with no damping, and the crosses are the numerical results with a diffuse radial cutoff.

where A, B, and C are independent of ν, and given by Eq. (30). The value of $y_{\text{sph av}}$ can be stated for several different cases: If $T < 0$, where $T = B^2 - 4AC$, or $|\nu_{\pm}| > 1$, where $\nu_{\pm} = -B/2A \pm \sqrt{T}/2|A|$, then

$$y_{\text{sph av}} = [F(1) - F(-1)] \theta(V), \qquad (38)$$

with $V = A - B + C$ and $F(\nu) = A\nu^3/6 + B\nu^2/4 + C\nu/2$. If $|\nu_+| > 1$ but $|\nu_-| < 1$, then

$$y_{\text{sph av}} = [F(\nu_-) - F(-1)] \theta(V) + [F(1) - F(\nu_-)] \theta(-V). \qquad (39)$$

If $|\nu_-| > 1$ but $|\nu_+| < 1$, then

$$y_{\text{sph av}} = [F(\nu_+) - F(-1)] \theta(V) + [F(1) - F(\nu_+)] \theta(-V). \qquad (40)$$

Finally, if $|\nu_{\pm}| < 1$, then

$$y_{\text{sph av}} = [F(\nu_-) - F(-1) + F(1) - F(\nu_+)] \theta(V)$$
$$+ [F(\nu_+) - F(\nu_-)] \theta(-V). \qquad (41)$$

III. CORRELATION HOLE

The local density $n(\mathbf{r})$ sets only one length scale for exchange (the Fermi wavelength) but it sets a second for correlation, the Thomas-Fermi screening length. Since the correlation hole is *not* required to satisfy a negativity constraint like Eq. (8), we do not need the non-spherical component of its GEA density. We write the spherically averaged GEA correlation hole as

$$n_c^{\text{GEA}}(\mathbf{r}, u) = n_c^{\text{LSD}}(r_s, \zeta, v) + t^2 \delta n_c(r_s, \zeta, v), \qquad (42)$$

where

$$v = \phi k_s u \qquad (43)$$

is the reduced electron-electron separation on the scale of the screening length.

The LSD correlation hole function $n_c^{\text{LSD}}(r_s, \zeta, v)$ is accurately known,[15] and has been confirmed by recent quantum Monte Carlo calculations.[54] We write

$$n_c^{\text{LSD}}(r_s, \zeta, v) = \phi^5 k_s^2 A_c(r_s, \zeta, v), \qquad (44)$$

where (for $r_s \leq 10$)

$$4\pi v^2 A_c(r_s, \zeta, v) = f_1(v) + f_2(r_s, \zeta, v). \qquad (45)$$

Here $f_1(v)$ is a nonoscillatory long-range contribution, known from the random phase approximation (RPA). [Correction to Eq. (22) of Ref. 15: $a_3 = 0.002\ 431\ 7$]. The short-range contribution $f_2(v)$ vanishes rapidly for $v \gg 1/\sqrt{p}$, where

$$p(r_s, \zeta) = \pi k_F d(\zeta)/4\phi^4 \qquad (46)$$

and $d(\zeta) = 0.305 - 0.136\zeta^2$.

Similarly, we write the GEA correlation hole as

$$\delta n_c(r_s, \zeta, v) = \phi^5 k_s^2 B_c(r_s, \zeta, v), \qquad (47)$$

$$B_c(r_s, \zeta, v) = B_c^{\text{LM}}(v)[1 - \exp(-pv^2)]$$
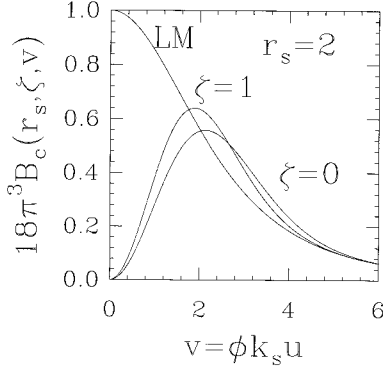$$+ \beta(r_s, \zeta) v^2 \exp(-pv^2), \qquad (48)$$

FIG. 4. The function $B_c(r_s,\zeta,v)$, which defines the shape of the gradient correction to the correlation hole via Eq. (48), for $r_s=2$ with $\zeta=0$ and $\zeta=1$. Also shown is the entire Langreth-Mehl ($r_s=\zeta=0$) curve.

where

$$B_c^{LM}(v)=[18\pi^3(1+v^2/12)^2]^{-1} \qquad (49)$$

is the nonoscillating long-range contribution, the Fourier transform of the Langreth-Mehl[55] (LM) exponential model for the wave-vector decomposition of the gradient contribution to the correlation hole in the RPA.

Equation (48) contains no constant or linear term in v, so it does not alter the highly accurate LSD on-top hole or its cusp. The coefficient $\beta(r_s,\zeta)$ is determined from the known GEA correction to the energy, for which we use the Langreth-Mehl approximation to the high-density ($r_s\rightarrow 0$) limit, with the spin dependence of Ref. 56:

$$\Delta E_c^{GEA}=C_c^{LM}\int d^3r \; \phi(\zeta)|\nabla n|^2/n^{4/3}$$

$$=16(3/\pi)^{1/3}C_c^{LM}\int d^3r \; n\phi^3t^2, \qquad (50)$$

where $C_c^{LM}=(\pi/3)^{1/3}/(24\pi^2)$ differs only slightly from the exact high-density limit of Ma and Brueckner,[6] $\beta(\pi/3)^{1/3}/16$. Requiring our GEA correlation hole to recover this energy fixes

$$\beta(r_s,\zeta)=\frac{2p^2}{3\pi^2}[1-E_1(12p)], \qquad (51)$$

where $E_1(x)=x\;\exp(x)\int_x^\infty dt\;\exp(-t)/t$. Figure 4 shows both the Langreth-Mehl B_c and how the short-range contribution changes it for $r_s=2$ and $\zeta=0,1$.

A key fact is that Eq. (47) and its normalization integral are well defined but positive. While the LSD correlation hole properly integrates to zero, the GEA correlation hole does not.[21] A simplification is that A_c of Eq. (45) and B_c of Eq. (48), which are functions of three variables, correctly reduce to functions of v alone in either the high-density ($r_s\rightarrow 0$, $p\rightarrow\infty$) or the long-range ($v\rightarrow\infty$) limits, where RPA is valid.

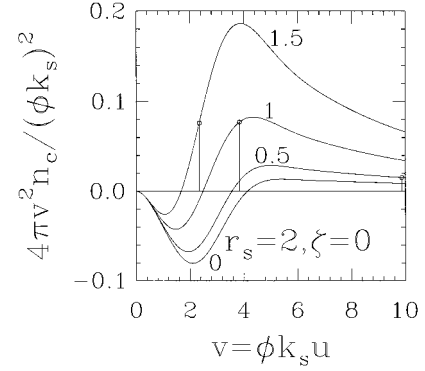With the GEA correlation hole fully defined, we construct the spherically averaged GGA hole

FIG. 5. Spherically averaged correlation hole density n_c for $r_s=2$ and $\zeta=0$. GEA holes are shown for four values of the reduced density gradient, $t=|\nabla n|/(2k_\zeta n)$. The vertical lines indicate where the numerical GGA cuts off the GEA hole to make $\int_0^{v_c}dv \; 4\pi v^2 n_c(v)=0$.

$$n_c^{GGA}(r_s,\zeta,t,v)=\phi^5k_s^2[A_c(r_s,\zeta,v)+t^2B_c(r_s,\zeta,v)]$$

$$\times\theta(v_c-v), \qquad (52)$$

where $v_c(r_s,\zeta,t)$ is the largest root satisfying the normalization condition

$$\int_0^{v_c}dv \; 4\pi v^2[A_c(r_s,\zeta,v)+t^2B_c(r_s,\zeta,v)]=0. \quad (53)$$

Figure 5 is a plot of the spherically averaged GGA correlation hole for $r_s=2$ and $\zeta=0$ for several different values of t. We see that, for a small value of t ($t=0.5$), the gradient correction to LSD is small and so v_c is large (≈ 10.0), tending to its GEA value (∞) as $t\rightarrow 0$. On the other hand, for $t=1.5$, the gradient correction is 9 times larger, causing the cutoff to occur at a much smaller value of v_c ($v_c=2.3$). In the limit $t\rightarrow\infty$, $v_c\rightarrow 0$ (Fig. 6), turning off the correlation contribution altogether [as in Eq. (25)]. In all cases, the GGA correlation hole is more localized than either the LSD or GEA holes.

In Fig. 6, we follow v_c as a function of t for $r_s=2$, for both the spin-unpolarized ($\zeta=0$) and the fully spin-polarized
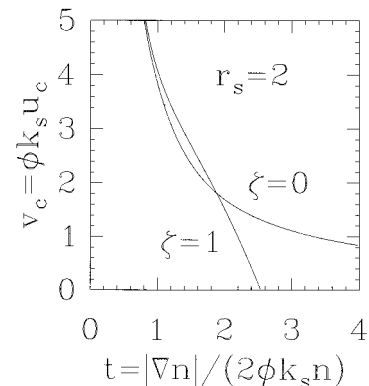

FIG. 6. Reduced cutoff separation for the GGA correlation hole, for $r_s=2$ and $\zeta=0$ or $\zeta=1$. For $\zeta=1$, $v_c=0$ beyond $t\approx 2.5$. For the case $r_s=2$ and $\zeta=0$, $u_c\lesssim r_s$ means $t\gtrsim 1.4$ and $s\gtrsim 1.6$.
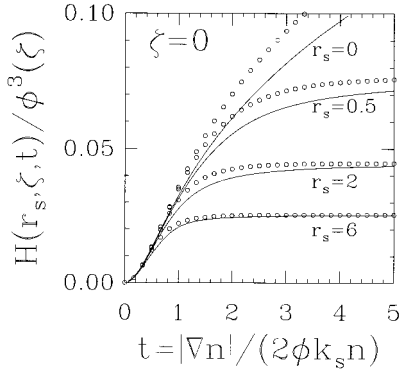
FIG. 7. The function $H = \epsilon_c^{\mathrm{GGA}} - \epsilon_c^{\mathrm{LSD}}$ for several values of r_s for the spin-unpolarized case ($\zeta = 0$). The solid lines are the numerical result of the real-space cutoff procedure, while the open circles are from the PBE parametrization of Eq. (22).

($\zeta = 1$) cases. Note that, for small t, v_c is large, and the curves ($\zeta = 0$ or 1) merge because the long-range contribution to the hole is independent of ζ. The same qualitative behavior occurs for all densities, although for higher densities ($r_s \to 0$) the short-range contribution becomes negligible for all t and the two curves become everywhere identical.

The GGA correlation energy per particle at position **r** is now

$$\epsilon_c^{\mathrm{GGA}}(r_s, \zeta; t) = \phi^3 \int_0^{v_c} dv \, \frac{4\pi v^2}{2v} [A_c(r_s, \zeta, v) + t^2 B_c(r_s, \zeta, v)]$$

$$= \epsilon_c^{\mathrm{unif}}(r_s, \zeta) + H(r_s, \zeta, t). \qquad (54)$$

In Fig. 7, we plot the difference between the GGA and LSD correlation energies for different values of r_s, as a function of t for the spin-unpolarized case ($\zeta = 0$). For $t^2 \to 0$, this figure recovers the t^2 behavior of GEA. Since the GGA correlation energy vanishes at large gradients, the limit as $t \to \infty$ in this figure is precisely $-\epsilon_c^{\mathrm{unif}}$. Figure 8 shows the same for $\zeta = 1$. Figures 7 and 8 also show the fair agreement between the analytic PBE expression of Eq. (22) and the numerical GGA. The results for PW91 are very similar, except that as $r_s \to 0$, $H^{\mathrm{PW91}}(t)$ becomes a simple parabola for large t, due to the H_1 term in that functional.[23]

Finally, compare Figs. 7 and 8 to deduce an approximate spin-scaling relationship for $r_s \lesssim 6$:

$$\epsilon_c^{\mathrm{GGA}}(r_s, \zeta; t) \approx \phi^3(\zeta) \epsilon_c^{\mathrm{GGA}}(r_s, 0; t/\phi(\zeta)). \qquad (55)$$

IV. QUALITATIVE FEATURES OF THE GGA HOLES

At the LSD level, our models are essentially exact. The only missing ingredient is the large-u oscillation of the correlation hole, which is energetically unimportant[15] and is washed away in the average of Eq. (7). When the reduced gradient s of Eq. (14) vanishes at the position of the electron, our GGA holes reduce to LSD, and so are fixed by the local value of r_s. In the high-density ($r_s \to 0$) limit, the exchange hole exists on a length scale $\propto r_s$, while the correlation hole
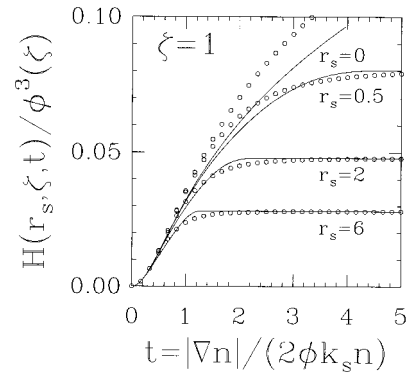

FIG. 8. Same as Fig. 7, but for the fully spin-polarized case ($\zeta = 1$).

is diffused over a much greater length scale $\propto \sqrt{r_s}$, and each displays a simple scaling behavior. Thus exchange dominates correlation: $\epsilon_x^{\mathrm{unif}} \propto r_s^{-1}$ and $\epsilon_c^{\mathrm{unif}} \propto \ln(r_s)$. As r_s increases, the exchange hole expands more rapidly than the correlation hole, and ultimately engulfs it. In the low-density ($r_s \to \infty$) limit, the exchange and correlation holes each scale with r_s and are of comparable size. The extreme long-range part of the correlation hole is always given by RPA, as is the $r_s \to 0$ limit.

The gradient corrections to the hole are known less reliably than the LSD terms. Second-order gradient corrections to the LSD on-top hole and cusp are small[18] and neglected here. In fact, self-consistent LSD or GGA calculations provide accurate predictions[57,58] for $n(\mathbf{r})$ and $n_{xc}(\mathbf{r}, \mathbf{r})$, even when symmetry breaking leads to serious errors in $\zeta(\mathbf{r})$ of Eq. (18). The gradient corrections display the same small- and large-r_s scalings as do the LSD holes.

A nonzero reduced gradient s at the position of the electron affects the holes at small u, deepening the exchange part and raising the correlation part. The large-u contributions to the GGA holes are chopped off. This leads to the scaling limit of Eq. (26), since $r_s(\mathbf{r}) \to \gamma^{-1} r_s(\gamma \mathbf{r})$, $s(\mathbf{r}) \to s(\gamma \mathbf{r})$, and $t(\mathbf{r}) \to \gamma^{1/2} t(\gamma \mathbf{r})$ under uniform scaling.

As the reduced gradient s increases, the exchange hole [constrained by Eqs. (5) and (8)] becomes deeper and more short ranged in u, so the negative exchange energy turns on more strongly. But the correlation hole [constrained by Eq. (6)] is gradually cut down to zero, so the correlation energy turns off. All these effects may be seen in the GGA exchange and correlation energies, as depicted in Figs. 3, 7, and 8, and in Fig. 1 of Ref. 30; see also Refs. 52 and 59.

[1] W. Kohn and L.J. Sham, Phys. Rev. **140**, A1133 (1965).

[2] R.O. Jones and O. Gunnarsson, Rev. Mod. Phys. **61**, 689 (1989).

[3] R.G. Parr and W. Yang, *Density Functional Theory of Atoms and Molecules* (Oxford, New York, 1989).

[4] R.M. Dreizler and E.K.U. Gross, *Density Functional Theory* (Springer-Verlag, Berlin, 1990).

[5] J.P. Perdew and Y. Wang, Phys. Rev. B **45**, 13 244 (1992).

[6] S.-K. Ma and K.A. Brueckner, Phys. Rev. **165**, 18 (1968).

[7] L.J. Sham, in *Computational Methods in Band Theory*, edited by P.M. Marcus, J.F. Janak, and A.R. Williams (Plenum, New York, 1971), p. 458.

[8] M. Rasolt and H.L. Davis, Phys. Lett. **86A**, 45 (1981).

[9] M. Rasolt and D.J.W. Geldart, Phys. Rev. B **34**, 1325 (1986).

[10] L. Kleinman and S. Lee, Phys. Rev. B **37**, 4634 (1988).

[11] D.C. Langreth and S.H. Vosko, Adv. Quantum Chem. **21**, 175 (1990).

[12] J.P. Perdew and Y. Wang, Phys. Rev. B **33**, 8800 (1986); **40**, 3399(E) (1989).

[13] J.P. Perdew, Phys. Rev. B **33**, 8822 (1986); **34**, 7406(E) (1986).

[14] O. Gunnarsson and B.I. Lundqvist, Phys. Rev. B **13**, 4274 (1976).

[15] J.P. Perdew and Y. Wang, Phys. Rev. B **46**, 12 947 (1992).

[16] M. Ernzerhof, J.P. Perdew, and K. Burke, in *Density Functional Theory*, edited by R. Nalewajski (Spinger-Verlag, Berlin, 1996).

[17] J.P. Perdew, Phys. Rev. Lett. **55**, 1665 (1985); **55**, 2370(E) (1985).

[18] K. Burke, M. Ernzerhof, and J.P. Perdew (unpublished).

[19] K. Burke, J.P. Perdew, and D.C. Langreth, Phys. Rev. Lett. **73**, 1283 (1994).

[20] K. Burke and J.P. Perdew, Int. J. Quantum Chem. **56**, 199 (1995).

[21] D.C. Langreth and J.P. Perdew, Phys. Rev. B **21**, 5469 (1980).

[22] Y. Wang, J.P. Perdew, J.A. Chevary, L.D. MacDonald, and S.H. Vosko, Phys. Rev. A **41**, 78 (1990).

[23] J.P. Perdew, in *Electronic Structure of Solids '91*, edited by P. Ziesche and H. Eschrig (Akademie Verlag, Berlin, 1991), p. 11.

[24] A.D. Becke, J. Chem. Phys. **98**, 5648 (1993).

[25] M. Ernzerhof, Chem. Phys. Lett. (to be published); K. Burke, M. Ernzerhof, and J. P. Perdew, *ibid.* (to be published); J. P. Perdew, M. Ernzerhof, and K. Burke, J. Chem. Phys. (to be published).

[26] J.P. Perdew, J.A. Chevary, S.H. Vosko, K.A. Jackson, M.R. Pederson, D.J. Singh, and C. Fiolhais, Phys. Rev. B **46**, 6671 (1992); **48**, 4978(E) (1993).

[27] A.D. Becke, Phys. Rev. A **38**, 3098 (1988).

[28] B.G. Johnson, P.M.W. Gill, and J.A. Pople, J. Chem. Phys. **98**, 5612 (1993).

[29] E. Engel and S.H. Vosko, Phys. Rev. B **47**, 13 164 (1993).

[30] J.P. Perdew, K. Burke, and M. Ernzerhof, Phys. Rev. Lett. (to be published).

[31] M. Levy, Int. J. Quantum Chem. **S23**, 617 (1989).

[32] K. Burke, J. P. Perdew, and Y. Wang (unpublished).

[33] C.J. Umrigar and X. Gonze, in *High Performance Computing and its Application to the Physical Sciences*, Proceedings of the Mardi Gras 1993 Conference, edited by D.A. Browne *et al.* (World Scientific, Singapore, 1993).

[34] M. Slamet and V. Sahni, Phys. Rev. B **44**, 10 921 (1991).

[35] K. Burke, J.P. Perdew, and M. Levy, in *Modern Density Functional Theory: A Tool for Chemistry*, edited by J.M. Seminario and P. Politzer (Elsevier, Amsterdam, 1995).

[36] A.D. Becke, J. Chem. Phys. **97**, 9173 (1992).

[37] J.C. Grossman, L. Mitas, and K. Raghavachari, Phys. Rev. Lett. **75**, 3870 (1995); **76**, 1006(E) (1996).

[38] D. Porezag and M.R. Pederson, J. Chem. Phys. **102**, 9345 (1995).

[39] E.I. Proynov, E. Ruiz, A. Vela, and D.R. Salahub, Int. J. Quantum Chem. **S29**, 61 (1995).

[40] A.C. Scheiner, J. Baker, and J.W. Andzelm, J. Comput. Chem. (to be published).

[41] A. Garcia, C. Elsässer, J. Zhu, S.G. Louie, and M.L. Cohen, Phys. Rev. B **46**, 9829 (1992); **47**, 4130(E) (1993).

[42] D.J. Singh and J. Ashkenazi, Phys. Rev. B **46**, 11 570 (1992).

[43] V. Ozolins and M. Körling, Phys. Rev. B **48**, 18 304 (1993).

[44] C. Filippi, D.J. Singh, and C. Umrigar, Phys. Rev. B **50**, 14 947 (1994).

[45] P. Dufek, P. Blaha, and K. Schwarz, Phys. Rev. B **50**, 7279 (1994).

[46] N.A.W. Holzwarth and Y. Zeng, Phys. Rev. B **49**, 2351 (1994).

[47] P. Söderlind, O. Eriksson, J.M. Willis, and B. Johannson, Phys. Rev. B **50**, 7291 (1994).

[48] N. Moll, M. Bockstedte, M. Fuchs, E. Pehlke, and M. Scheffler, Phys. Rev. B **52**, 2550 (1995).

[49] L. Stixrude and R.E. Cohen, Science **267**, 1972 (1995).

[50] B. Hammer and J.K. Nørskov, Nature **376**, 238 (1995).

[51] D.R. Hamann, Phys. Rev. Lett. **76**, 660 (1996).

[52] M. Levy and J.P. Perdew, Phys. Rev. B **48**, 11 638 (1993).

[53] A. Zupan, J.P. Perdew, K. Burke, and M. Causá, Int. J. Quantum Chem. Symp. (to be published).

[54] W.E. Pickett and J.Q. Broughton, Phys. Rev. B **48**, 14 859 (1993).

[55] D.C. Langreth and M.J. Mehl, Phys. Rev. B **28**, 1809 (1983).

[56] Y. Wang and J.P. Perdew, Phys. Rev. B **43**, 8911 (1991).

[57] J.P. Perdew, A. Savin, and K. Burke, Phys. Rev. A **51**, 4531 (1995).

[58] J.P. Perdew, M. Ernzerhof, K. Burke, and A. Savin, Int. J. Quantum Chem. (to be published).

[59] J.P. Perdew and K. Burke, Int. J. Quantum Chem. **57**, 309 (1996).